

## Review

# Smoke generation in black powder combustion

Mitsuo KOSHI\*<sup>†</sup>

\*Graduate School of Environmental and Information Sciences, Yokohama National University,  
79-7 Tokiwadai, Hodogaya-ku, Yokohama-shi, 240-8501 JAPAN

Phone: 03-3968-0233

<sup>†</sup>Corresponding author: koshim@jcom.home.ne.jp

Received: March 3, 2018 Accepted: April 19, 2018

## Abstract

In this study, a simple model for the smoke formation in black powder combustion is developed. Smoke formation is modeled as nucleation from gas phase molecules. The precursor molecules for this nucleation process for black powder with 75 wt% of  $\text{KNO}_3$  are identified as potassium salts such,  $\text{K}_2\text{CO}_3$  and  $\text{K}_2\text{SO}_4$ . This determination is based on the partial-equilibrium calculations in which chemical species in the condensed phase are excluded. Standard classical nucleation theory (CNT) is adopted to estimate the radius and formation rate of the critical nuclei of smoke particles. The main components of smoke from black powder are  $\text{K}_2\text{CO}_3$  or  $\text{K}_2\text{SO}_4$  particles, depending on the sulfur content. The predicted nucleation rates of the particles are very fast. The time variation of the averaged particle radius and volume fraction of smoke is also evaluated by solving the population balance equation (Smoluchowski equation). The volume fraction of smoke produced by black powder combustion is predicted to be of the order of  $10^{-4}$ .

This study also investigates how ammonium perchlorate ( $\text{NH}_4\text{ClO}_4$ , AP) added to the black powder affects smoke formation, using CNT and the Smoluchowski equation. CNT predicts that the critical radius of  $\text{K}_2\text{CO}_3$  and  $\text{K}_2\text{SO}_4$  particles can be considerably increased by the addition of AP to black powder. This intervention could thus reduce smoke-particle formation. Although CNT predicts that no KCl particles will form because of the high vapor pressure of KCl, the Smoluchowski equation indicates that KCl particles will be produced with a large amount of added AP. Solutions of the Smoluchowski equation also indicate that the average particle diameter and volume fraction of smoke decrease if the amount of added AP is increased.

**Keywords:** black powder, smoke formation, potassium salt, nucleation theory, Smoluchowski equation

## 1. Introduction

Smoke generated by explosive combustion of black powder reduces the visibility of aerial fireworks displays in calm weather. Therefore, fireworks designers strive to reduce the amount of smoke produced by their explosive charges. In general, the size of particles in smoke ranges from several nm to  $1\ \mu\text{m}$ . Particulate matter generated by fireworks displays also has a negative environmental impact. Many researchers have studied particle pollution from fireworks displays in recent years<sup>1)–5)</sup>. The atmospheric concentration of PM10 (particulate matter with a diameter less than  $10\ \mu\text{m}$ ) significantly increases during and after the aerial fireworks displays associated with various holidays and celebrations around the world. Camilleri and Vella<sup>6)</sup> measured PM10 emission factors for various pyrotechnic devices, namely, flash crackers, stars,

black powder blast charges, and fuse matches, as they are produced in Malta. The emission factor was defined as the total mass of PM10 divided by the mass of the explosive material in the pyrotechnic device. The PM10 emission factors were as follows, in kg per kg-composition: blast charges 0.054; flash crackers 0.43; stars 0.175 (red); 0.176 (blue); 0.254 (green); 0.123 (white); fuse matches 0.204. According to these results, black powder blast charges produce much less PM10 than other devices.

However, the particles in the smoke produced by combustion of black powder seem to have different origin than that of the PM10 detected in these air pollution studies. The diameters of smoke particles are usually less than  $1\ \mu\text{m}$ , much smaller than PM10, and the smoke is very rapidly produced. White smoke is often observed when black powder combusts with a flame. This white

smoke is thought to be composed of nanoparticles of  $K_2CO_3$  and  $K_2SO_4$ <sup>15)</sup>. To the best of our knowledge, no research group has studied the chemical and physical mechanism behind the very fast production of these very fine smoke particles from black powder combustion.

The present study aims to understand the kinetic mechanism behind the formation of fine particles in black powder combustion, to allow control of the size and rate of particles so that aerial display fireworks remain visible even in calm weather. To this end, we developed a simple model to predict the size and production rate of particles from black powder combustion.

In this study, the smoke formation is modeled as nucleation of gas-phase molecules. Standard classical nucleation theory (CNT) is adopted to estimate the radii and formation rate of critical nuclei of smoke particles. Time variations of the average particle radius and volume fraction of smoke are evaluated by solving the population-balance Smoluchowski equation. Details of the model and the computational methods used are described in Section 2. The model is used to predict the size and the generation rate of smoke particles in black powder combustion in Section 3. Strategies for the reduction of smoke in black powder combustion are briefly discussed in Section 4. Conclusions and future work are discussed in Section 5.

## 2. Theories for smoke particle growth

Two different theoretical methods are employed in this study to estimate the size of smoke particles and their nucleation rates. This section briefly outlines the two theories.

### 2.1 Classical nucleation theory (CNT)

CNT is a widely used model for understanding the formation of new thermodynamic phases, such as liquid or solid phases forming from gaseous material<sup>7), 8)</sup>. Although CNT is an approximate model, it gives reasonable predictions of nucleation rates. CNT is based on the condensation of vapor into liquid. The change in the free energy of the system during the homogeneous formation of spherical nuclei with radius  $r$  is given by

$$\Delta G = -\frac{4\pi r^3}{3\nu_1} k_B T \ln \xi + 4\pi r^2 \sigma. \quad (1)$$

Here,  $\nu_1$  is the volume of a single molecule in liquid or solid phase,  $\xi = P/P_{eq}$  is the vapor-supersaturation ratio,  $P_{eq}$  is the equilibrium vapor pressure,  $k_B$  is the Boltzmann constant, and  $\sigma$  is the specific surface energy of the interface between droplets and the surrounding vapor. In conventional CNT, this surface energy is assumed to be equal to the surface tension of a flat surface of the liquid (or solid). This feature is known as the capillary assumption. The first term represents the energy decrease upon the transition from vapor to liquid and this term is dominant for nuclei with relatively large  $r$ . When  $r$  is relatively small, the second term is dominant. This term represents the free energy released by the creation of a new surface. Thus, the two terms in Equation (1) differently depend on  $r$ , and therefore the free energy  $\Delta G$

of nucleus formation passes through a maximum at  $r = r^*$ .  $r^*$  is the critical radius at which the probability of nucleation passes through a minimum (critical radius). If the nucleus radius is larger than  $r^*$ , nucleation is spontaneous since the free energy needed to form larger nuclei is less than the free energy at this radius. The value of  $r^*$  can be found by differentiating Equation (1) with respect to  $r$ :

$$r^* = \frac{2\sigma\nu_1}{k_B T \ln \xi}. \quad (2)$$

The free energy at  $r = r^*$  is given as:

$$\Delta G^* = \frac{16\pi\sigma^3\nu_1^2}{3k_B^2 T^2 (\ln \xi)^2}. \quad (3)$$

The nucleation rate  $J$  per unit time can be expressed as follow:

$$J = A \exp\left[-\frac{\Delta G^*}{k_B T}\right]. \quad (4)$$

The pre-exponential factor  $A$  is determined by kinetic considerations and given as<sup>9)</sup>:

$$A = \frac{1}{3} z s_1 \left(\frac{\theta}{\pi}\right)^{1/2}. \quad (5)$$

Here,  $s_1$  is the surface area of a single molecule in condensed phase and  $z$  is the collision frequency:

$$z = \left(\frac{k_B T}{2\pi m}\right)^{1/2} N_g. \quad (6)$$

$m$  is mass of the molecule and  $N_g$  is number density of gas-phase molecule ( $N_g = P/k_B T$ ).  $\theta$  in Equation (5) is defined by:

$$\theta = \frac{\sigma s_1}{k_B T}. \quad (7)$$

With Equations (1)–(7), the minimum particle size and the nucleation rate can be evaluated.

### 2.2 Smoluchowski equation and the sectional method

Smoke particles of potassium salts will be produced from gas-phase products of black powder combustion. We assume that smoke particles are produced by the particle-inception reaction of gas-phase potassium salts. Particles produced in this fashion will then grow by coagulation and aggregation. Since coagulation simply redistributes the particle-size distribution, it does not affect the total mass of particles in the system. The following basic assumptions about coagulation are imposed in our model:

- (i) Primary particles are all spherical.
- (ii) Colliding particles immediately coalesce into new spherical particles.
- (iii) Mass and volume are conserved by the coagulation.

According to these assumptions, the following relations are valid for smoke particle of class  $i$ , defined as the particle composed of  $i$ -monomer chemical species:

$$m_i = i \cdot m_1, V_i = i \cdot V_1, \quad (8)$$

$$D_i = (6V_i/\pi)^{1/3} = i^{1/3} D_1, \quad (9)$$

$$V_i + V_j = V_{i+j} = (i+j) V_1, N_i + N_j = N_{i+j}. \quad (10)$$

Here,  $m_i$ ,  $V_i$ ,  $D_i$ , and  $N_i$  are mass, volume, diameter and number density of particle of class  $i$ , respectively.

The net rate of generation of class- $i$  smoke particles is described by the Smoluchowski population-balance equation<sup>10</sup>, which is written as:

$$\frac{dN_i}{dt} = -N_i \sum_{j=1}^{\infty} \beta_{1j} N_j, \quad (11a)$$

$$\frac{dN_i}{dt} = \frac{1}{2} \sum_{j=1}^{i-1} \beta_{jj-1} N_j N_{i-j} - N_i \sum_{j=1}^{\infty} \beta_{ij} N_j, (i = 2, 3, \dots). \quad (11b)$$

Here,  $\beta_{ij}$  is the collision frequency between particle of class  $i$  and class  $j$ .

The functional form of the collision frequency  $\beta_{ij}$  depends on the physical model employed for coagulation. Particle coagulation is classified by the Knudsen number,  $K_n = 2\lambda/D$ , where  $\lambda$  is the mean free path of the surrounding gas and  $D$  is the diameter of the particle. For the regime with free molecules ( $K_n \gg 1$ ), the collision frequency is expressed as

$$\beta_{ij} = \sqrt{\frac{\pi k_B T}{2\rho_p}} \sqrt{\frac{1}{V_i} + \frac{1}{V_j}} (D_i + D_j)^2, \quad (12)$$

Here,  $\rho_p$  is the particle density. In the continuum coagulation regime ( $K_n \ll 1$ ), the collision frequency is given as

$$\beta_{ij} = \frac{2k_B}{3} \frac{(D_i + D_j)^2}{D_i D_j} \frac{T}{\eta}. \quad (13)$$

$\eta$  is gas viscosity. Coagulation occurring between the free-molecule and continuum regimes ( $K_n \approx 1$ ) is referred to as the transition regime. The collision frequency in this regime can be represented by an interpolating polynomial implemented in Chemkin-Pro<sup>11</sup>.

In this study, the Smoluchowski equation, Equation (11), was solved by the sectional method as implemented in ANSYS Chemkin-pro 18.1<sup>11</sup>. The particle-size domain is divided into a finite number of sections in this method. The sectional method in Chemkin is based on the discretized population balance developed by Litster et al.<sup>12</sup> and Kumar and Ramkrishna<sup>13</sup>. This sectional method ensures correct prediction of the total particle number and volume. The particle-size distribution is discretized by geometric, adjustable sections as follows:

$$\frac{V_{i+1}}{V_i} = 2^{1/q} \quad (14)$$

Here,  $q$  is a positive integer, and  $V$  is the volume (class), and subscript  $i$  is the section index. The higher value of  $q$  gives the finer resolution.

Aggregation and coagulation modify the particle-size distribution. The term aggregation is used for non-coalescing collisions. Particle-particle aggregation processes can be modeled as a sequence of collision, sticking, and sintering processes. The parameters for these processes in the case of smoke particles produced by

black powder combustion are unknown. Therefore, in this study, we use a simple model for aggregation with the following assumptions:

- (iv) All primary particles are spherical.
- (v) All primary particles in an aggregate are of the same size.
- (vi) Aggregates with primary particles less than the limiting value,  $D_{limit}$ , can be thought of as completely coalesced spheres. Aggregates with larger primary particles are pure aggregates in which primary particles of the limiting size are in point contact with each other.
- (vii) The collision diameter of each aggregate of class  $j$  is given as:

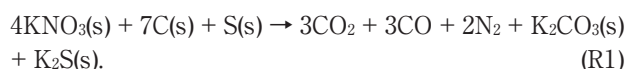
$$D_{cj} = \left( \frac{6}{\pi} \frac{N_j V_j}{N_{pj}} \right)^{1/3} \left( \frac{N_{pj}}{N_j} \right)^{1/D_f} \quad (15)$$

In Equation (15), subscripts  $p$  and  $j$  indicate primary particle and the class (i.e., the number of chemical species) of the aggregate, respectively, and  $D_f$  is the mass fractal dimension. Only the parameters  $D_{limit}$  and  $D_f$  need to be specified in this simple model. This simple aggregation model is available in ANSYS Chemkin-pro and was used to generate the results described below.

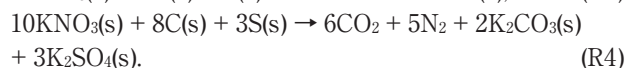
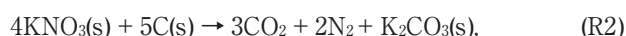
### 3. Smoke generation in black powder combustion

#### 3.1 Combustion of black powder

Black powder is composed of potassium nitrate ( $\text{KNO}_3$ ), carbon (C), and sulfur (S). The products of black powder combustion differ according to the composition of the black powder. The stoichiometry of a typical black powder preparation containing  $\text{KNO}_3$  (77 mole %), charcoal (17 mole %), and sulfur (6 mole %) can be represented by the following equation<sup>14</sup>:



Another stoichiometry is also possible:



Here, (s) indicates that the species is in the solid state. Solid-state products of  $\text{K}_2\text{CO}_3(\text{s})$ ,  $\text{K}_2\text{S}(\text{s})$ , and  $\text{K}_2\text{SO}_4(\text{s})$  can be the source of the particles produced by black powder combustion. The actual processes of particulate production are extremely complex<sup>14,15</sup>. Multi-phase chemical reactions as well as a range of physical and chemical processes including vaporization, sublimation, coagulation, aggregation, and sintering are involved. As a starting point for discussion, chemical equilibrium calculations were performed with a program developed by Gordon and McBride (CEA400)<sup>16</sup>. Figure 1 depicts an example of the equilibrium calculations. Constant pressure ( $P = 1$  bar) and adiabatic conditions are assumed ( $HP = \text{constant}$ ).

The mass fraction of  $\text{KNO}_3$  is fixed at  $Y(\text{KNO}_3) = 0.75$

wt% and the mass fraction of sulfur is varied from  $Y(S) = 2.5$  to 22.5 wt%. (Accordingly, the mass fraction of carbon is given by  $Y(C) = 25 - Y(S)$  wt%.) The adiabatic flame temperature increases from 1259 K ( $Y(S) = 2.5$  wt%) to 1955 K ( $Y(S) = 22.5$  wt%). This is because some of the sulfur acts as an oxidizer to yield liquid or solid  $K_2S^{15)}$ . The composition of combustion products largely depends on the mass fraction of sulfur. With low sulfur content ( $< 5$  wt%), the main products are CO,  $N_2$ ,  $K_2CO_3(l)$ , and  $K_2S(l)$ , while  $SO_2$ ,  $N_2$ , K, and  $K_2SO_4(l)$  are the main products with a

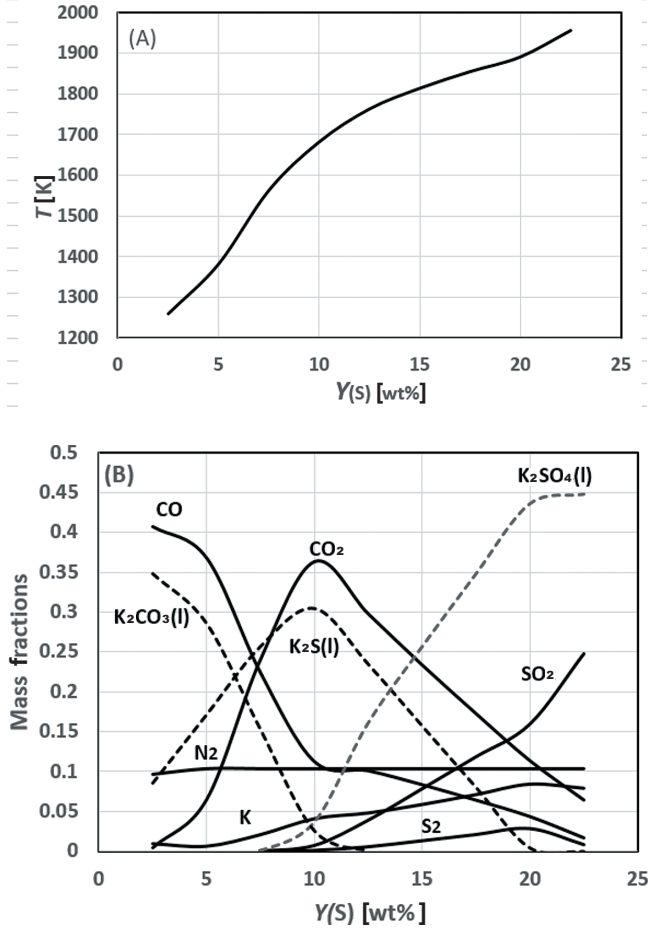
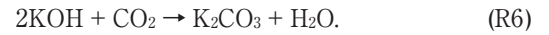


**Figure 1** Equilibrium temperature (A) and compositions (B) of black powder combustion at constant pressure ( $p = 1$  bar) and adiabatic condition as a function of mass fraction of sulfur,  $Y(S)$ . Mass fraction of  $KNO_3$  is fixed to  $Y(KNO_3) = 75$  wt%.

high sulfur content ( $> 20$  wt%). The typical black powder recipe of  $KNO_3/C/S = 75/15/10$  wt% gives the main products of  $CO_2$ , CO,  $N_2$ , and  $K_2S(l)$ . Here (l) indicates liquid products.

These liquid products will yield solid residuals after they are cooled down by mixing with the ambient air. These combustion products in the condensed phase are likely one source of particulate matter (PM). However, particulate generation from the liquid phase is slow since it involves the breakup of liquid droplets and cooling by mixing with ambient air. In addition, the size of particles produced by this path will be rather large ( $> 1 \mu m$ ). On the other hand, smoke particles are produced in a very short period and at sizes of the order of the wavelength of visible light ( $< 1 \mu m$ ). Such small particles may be produced by nucleation of gas-phase molecules. The nuclei so formed will grow very quickly into the small PM in smoke. A schematic of particle formation in black powder combustion is depicted in Figure 2.

Ignition of black powder starts with the melting of ingredients<sup>14)</sup>. Exothermic reactions in the liquid will produce  $K_2CO_3(l)$ ,  $K_2S(l)$ , and  $K_2SO_4(l)$ . Some part of these liquid products may form droplets and these droplets will break up into smaller droplets. However, nanoparticles cannot be formed by these breakup processes. Too many breakup steps are required to reach nanometer-size particles. Some other portion of the liquid products is cooled down to form solid residuals. The melting liquid also emits volatile gas-phase molecules, and gas-phase reactions will produce  $K_2CO_3$  and  $K_2SO_4$  gas molecules. For example,  $K_2CO_3$  can form by the following gas-phase reactions<sup>17)</sup>:



$K_2CO_3$  molecule was actually detected by mass spectrometry in the gas phase<sup>18)</sup>.

Note that the color of smoke generated by black powder combustion is white and practitioners generally believe<sup>15)</sup> that this smoke is composed of particles of  $K_2CO_3$ ,  $K_2SO_4$  and  $K_2S$ . Nanometer-size particles can be produced by nucleation from gas-phase  $K_2CO_3$  and  $K_2SO_4$  molecules. However, to the best of our knowledge, evidence for the

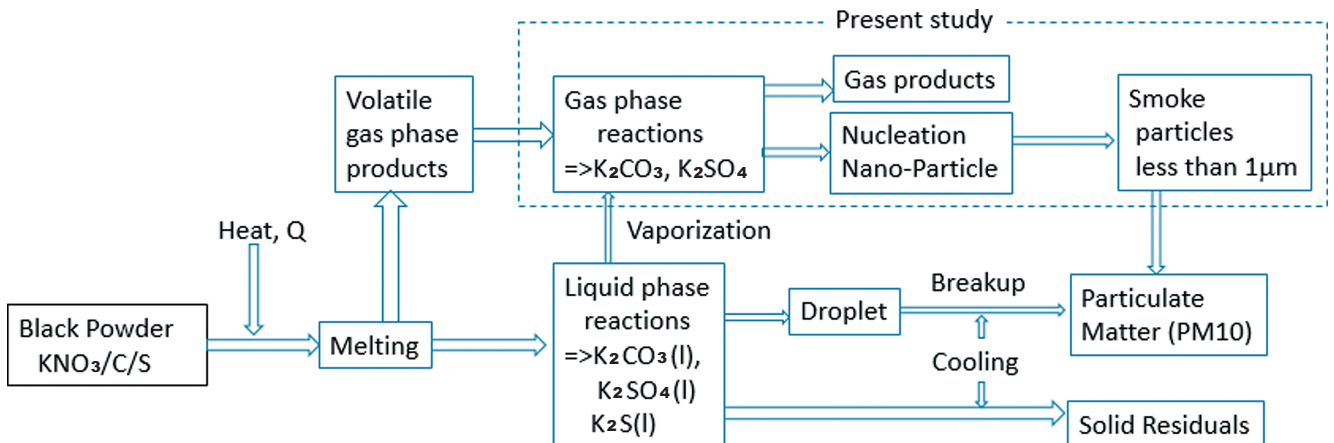


**Figure 2** Schematic diagram for particle formation in black powder combustion.



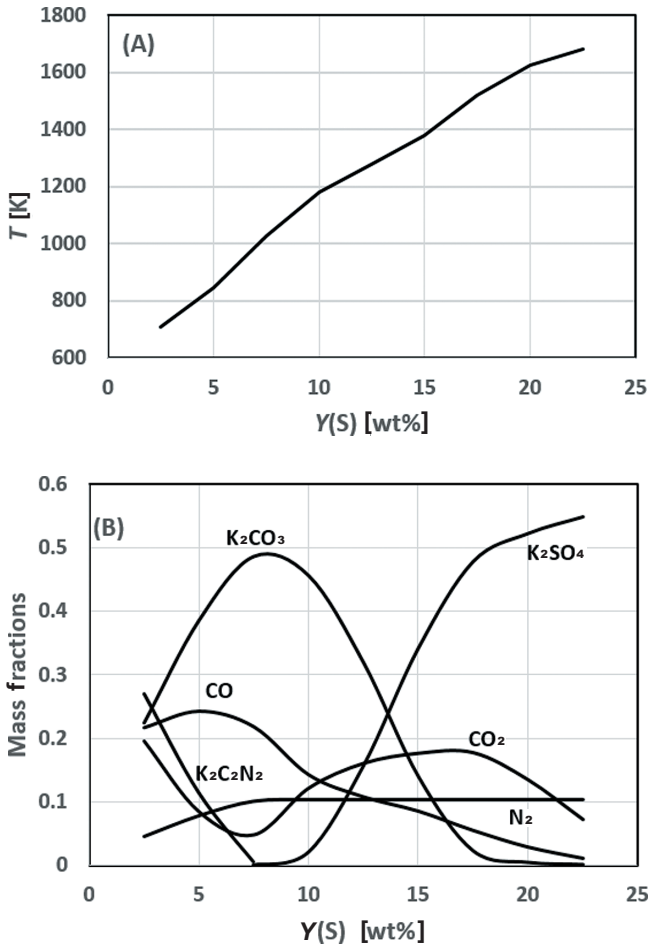


**Figure 3** Partial equilibrium temperature (A) and compositions (B) of black powder combustion at constant pressure ( $p=1\text{bar}$ ) and adiabatic condition as a function of mass fraction of sulfur,  $Y(S)$ . Mass fraction of  $KNO_3$  is fixed to  $Y(KNO_3) = 75\text{ wt\%}$ . Chemical species in condensed phase are excluded in this calculation.

existence of gas-phase  $K_2S$  molecules has not been reported in the literature. Future study is required to understand the chemical kinetic processes for  $K_2S$  nano-size clusters in smoke if they exist.

To predict the particle size (the critical radius for particle growth) and production rate, we must estimate the concentrations of gas-phase  $K_2CO_3$  and  $K_2SO_4$ . Partial-equilibrium calculations accomplish this estimation, wherein the Gibbs free energy is minimized while neglecting all condensed chemical species. The results of these partial-equilibrium calculations are depicted in Figure 3. The black powder recipe is the same as that in Figure 1. The partial-equilibrium temperatures are considerably lower than full-equilibrium temperatures. The lack of condensed-phase species results in this lower temperature since the formation of condensed-phase species is a highly exothermic process. The major species at partial equilibrium is  $K_2CO_3$  in sulfur-lean conditions and  $K_2SO_4$  in sulfur-rich conditions. Those gas-phase  $K_2CO_3$  and  $K_2SO_4$  molecules are converted into particles by nucleation.

### 3.2 Prediction of smoke generation based on classical nucleation theory

The vapor-supersaturation ratio,  $\xi = P/P_{eq}$ , is essential to determine the critical radius and nucleation rate with CNT, as discussed in Section 2.1. To evaluate  $\xi$ , the equilibrium vapor pressures are required. The vapor pressure,  $P_{eq}$ , can be calculated from the difference in chemical potential energy between the gas phase,  $\mu^0(g)$ , and condensed phase,  $\mu^0(l)$  or  $\mu^0(s)$ , as described in a standard physical chemistry textbook<sup>19)</sup>:

$$P_{eq} = \exp\left[\frac{\mu^0(l) - \mu^0(g)}{RT}\right] \text{ or } \exp\left[\frac{\mu^0(s) - \mu^0(g)}{RT}\right]. \quad (16)$$

$R$  is the universal gas constant. For the pure component, chemical potential energy is equal to standard molar Gibbs energy,  $G^0 = H^0 - TS^0$ . Standard enthalpy  $H^0$  and entropy  $S^0$  are expressed as a function of temperature with the following empirical equations in a NASA-CEA program package<sup>16)</sup>:

$$\frac{H^0(T)}{RT} = -a_1T^{-2} + a_2T^{-1} \ln T + a_3 + a_4\frac{T}{2} + a_5\frac{T^2}{3} + a_6\frac{T^3}{4} + a_7\frac{T^4}{5} + \frac{b_1}{T}, \quad (17)$$

$$\frac{S^0(T)}{R} = -a_1\frac{T^{-2}}{2} - a_2T^{-1} + a_3 \ln T + a_4T + a_5\frac{T^2}{2} + a_6\frac{T^3}{3} + a_7\frac{T^4}{4} + b_2. \quad (18)$$

The coefficients  $a_1 \sim a_7$ ,  $b_1$  and  $b_2$  for  $K_2CO_3$  and  $K_2SO_4$  in gas, liquid and solid phases are all given in a data base<sup>16)</sup>. The resulting vapor pressures are depicted in Figure 4.

Vapor pressure for  $K_2CO_3$  in bars can be expressed as:

$$\begin{aligned} \ln P_{eq}(K_2CO_3) &= -37691.96/T + 17.30 \quad 693K \leq T \leq 1173K, \\ &= -34268.21/T + 17.06 - 0.00233T \quad 1173K \leq T \leq 3000K, \end{aligned}$$

and for  $K_2SO_4$ :

$$\begin{aligned} \ln P_{eq}(K_2SO_4) &= -36487.3/T + 16.06 \quad 857K \leq T \leq 1342K, \\ &= -26462.6/T + 8.786 \quad 1342K \leq T \leq 3000K. \end{aligned}$$

The volume  $v_1$  and surface area  $s_1$  of a single molecule in the condensed phase can be calculated from the density. The temperature-dependent density of liquid  $K_2CO_3$  is given in Reference 20) as:

$$\rho(K_2CO_3) = 2.4141 - 4.421 \times 10^{-4}T, \quad [g\text{ cm}^{-3}]$$

No data is found for the liquid density of  $K_2SO_4$ . Density of solid  $K_2SO_4 = 2.66\text{ g cm}^{-3}$  is given in Reference 21), so the liquid density was approximated as:

$$\rho(K_2SO_4) = 2.66 - 6 \times 10^{-4}(T - T_m), \quad T \geq T_m \quad [g\text{ cm}^{-3}]$$

$T_m$  is the melting point ( $= 1342K$ ) of  $K_2SO_4$ .

The values for surface tension  $\sigma$  are taken from Reference 20):

$$\begin{aligned} \sigma(K_2CO_3) &= 273.71 - 0.06368T, \\ \sigma(K_2SO_4) &= 245.2 - 0.0443T, \quad [mN\text{ m}^{-1}] \end{aligned}$$

Using these values of vapor pressure, density and surface tension, it is possible to evaluate the critical radius and rate of nucleation if the partial pressures of  $K_2CO_3$  and

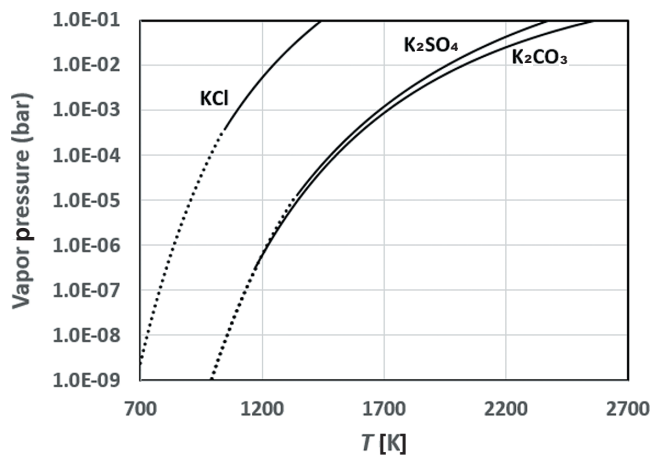


**Figure 4** Vapor pressures of  $\text{K}_2\text{CO}_3$ ,  $\text{K}_2\text{SO}_4$  and  $\text{KCl}$ . Dotted lines: solid, solid lines: liquid. (Melting point: 1173 K for  $\text{K}_2\text{CO}_3$ , 1342 K for  $\text{K}_2\text{SO}_4$ , and 1044 K for  $\text{KCl}$ )

$\text{K}_2\text{SO}_4$  are given. The supersaturation ratio,  $\xi$ , for  $\text{K}_2\text{CO}_3$  and  $\text{K}_2\text{SO}_4$  is evaluated at constant pressure (1 bar), under adiabatic conditions and the partial pressures given in Figure 3. The resulting critical radii and rates of nucleation are depicted in Figure 5.

The critical radius of  $\text{K}_2\text{CO}_3$  nuclei at  $Y(\text{S}) < 5$  wt% is less than 0.2 nm. The molecular radius of  $\text{K}_2\text{CO}_3$  is estimated to be 0.25 nm by quantum-chemical calculations at the B3LYP/CBSB7 level of theory using Gaussian-09 program package. Therefore, the value of  $r^* < 0.25$  nm is unrealistic. This indicates the limitation of the capillary approximation in CNT<sup>7)</sup>. For very small nuclei, the definition of surface tension in this model is very questionable and Equations (1) and (2) in the CNT are no longer valid. Such a small value of the critical radius is caused by an extremely large supersaturation ratio,  $\xi$ . As illustrated in Figure 3, the partial-equilibrium temperature at  $Y(\text{S}) < 5$  wt% is lower than the melting point of  $\text{K}_2\text{CO}_3$  ( $T_m = 1173$  K). As a result, the vapor pressure is very low and the value of  $\xi$  is very large. A very small value of  $r^*$  indicates a very rapid nucleation rate, as depicted in Figure 5 (B). However, the  $r^*$  value rapidly increases at  $Y(\text{S}) > 17$  wt% and the corresponding nucleation rate,  $J$ , sharply decreases. This trend predicts that smoke particles composed of  $\text{K}_2\text{CO}_3$  cannot be produced with a sulfur content higher than 17 wt%.

On the other hand, the nucleation of  $\text{K}_2\text{SO}_4$  exhibits the opposite trend. The critical radius is almost constant if  $Y(\text{S}) > 10$  wt%, and it gradually increases at  $Y(\text{S}) < 10$  wt%. This gradual increase in  $r^*$  is due to the very low partial pressure of  $\text{K}_2\text{SO}_4$  indicated in Figure 3. At the same time, the nucleation rate sharply decreases. This trend predicts that smoke particles composed of  $\text{K}_2\text{SO}_4$  cannot be produced with sulfur content lower than 12 wt%.

### 3.3 Prediction of smoke generation based on Smoluchowski equation

Although CNT can predict the critical radius of nucleation, it cannot evaluate the actual size of smoke particles. Once a critical nucleus is formed, the growth of

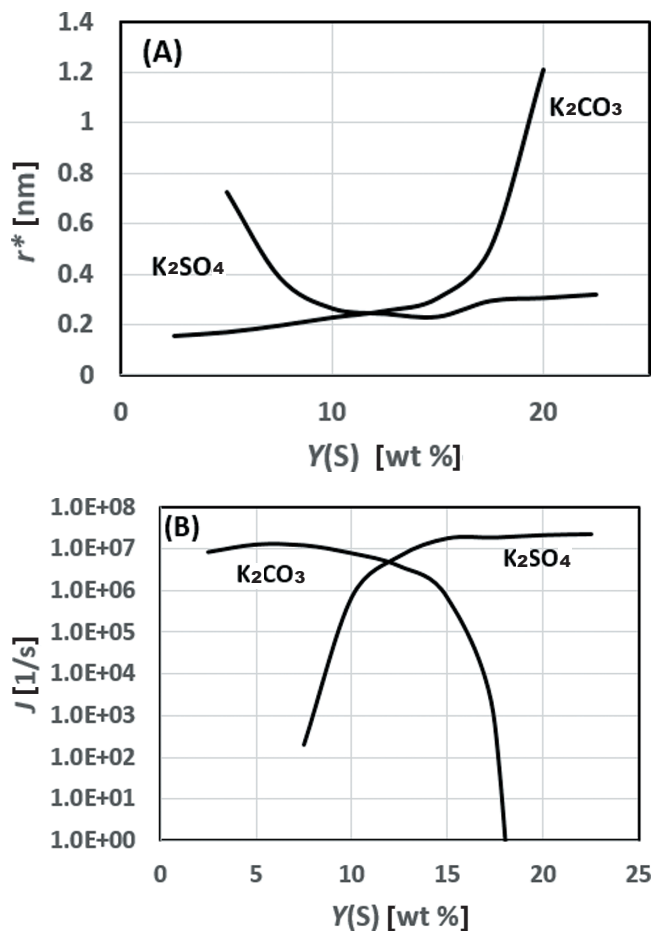


**Figure 5** Critical radius (A) and rate of nucleation,  $J$ , (B) for  $\text{K}_2\text{CO}_3$  and  $\text{K}_2\text{SO}_4$  in black powder combustion. Conditions are the same as in Figure 3.

the critical nucleus is spontaneous because the free energy decreases with increasing  $r$  if  $r > r^*$ . CNT can evaluate the value of  $r^*$ , but the nuclei formed at this threshold will grow as a function of time. To predict the actual size of the smoke particles, the kinetic equation for particle growth, i.e., the Smoluchowski equation in Equation (11), must be solved.

Within the simplified combustion model of black powder considered in this study, the initial conditions (temperature, pressure, and concentrations of precursor chemical species) in Equation (11) are given by the partial-equilibrium calculations described in Section 3.1. The precursor chemical species are the same as those identified by CNT, i.e.,  $\text{K}_2\text{CO}_3$  and  $\text{K}_2\text{SO}_4$ . Nucleation is the process of forming new condensed-phase particles from precursor gas-phase molecules. Particle inception is modeled as a nucleation reaction. This reaction is irreversible and all reactants must be gas-phase species. In this study, we assumed that the following nucleation reactions form  $\text{K}_2\text{CO}_3$  and  $\text{K}_2\text{SO}_4$  particles.



$\text{K}_2\text{CO}_3(\text{B})$  and  $\text{K}_2\text{SO}_4(\text{B})$  indicate bulk-phase (condensed-phase) particles composed of  $\text{K}_2\text{CO}_3$  and  $\text{K}_2\text{SO}_4$ , respectively. Note that the minimum particle size in Equation (11) is  $j = 2$  for these particle-inception reactions.

Collision frequencies are assumed for the following rate coefficients:

$$k_{R7} = 7.76 \times 10^{12} T^{0.5},$$

$$k_{R8} = 7.55 \times 10^{12} T^{0.5}. (\text{cm}^3 \text{mol}^{-1} \text{s}^{-1})$$

The sectional method was employed to solve Equation (11) with  $q = 1$  in Equation (14). The maximum number of sections is 40. For the aggregation model, no data is available for potassium-salt particles. Typical values for inorganic particles of  $D_{\text{limit}} = 30 \text{ nm}$  and  $D_f = 1.7$  are used as reasonable approximations in Equation (15).

Assuming that particle inception immediately begins after partial equilibrium is achieved, the time evolution of particle growth is calculated. A typical example of the calculation for  $\text{K}_2\text{CO}_3$  particle growth is depicted in Figure 6. In this example, the black powder recipe is  $\text{C/S/KNO}_3 = 15/10/75 \text{ wt\%}$  and the partial-equilibrium temperature of adiabatic, constant pressure (1 bar) combustion is  $T = 1181 \text{ K}$ . As depicted in Figure 6, particle inception is very rapid and the number density reaches a maximum within 10 ms and then rapidly decreases (Figure 6(A)). The average particle diameter is about 164 nm at  $t = 10 \text{ ms}$  and increases to 433 nm at  $t = 1 \text{ s}$ . Note that the volume fraction is nearly constant at  $1.43 \times 10^{-4}$  (Figure 6(C)). We, therefore, predict that black powder of this composition will produce a very large amount of  $\text{K}_2\text{CO}_3$  smoke particles.

Figure 7 depicts the average diameter and volume fraction of  $\text{K}_2\text{CO}_3$  and  $\text{K}_2\text{SO}_4$  particles as a function of  $Y(\text{S})$  with a fixed value of  $Y(\text{KNO}_3) = 75 \text{ wt\%}$  at reaction time  $t = 1 \text{ s}$ .  $\text{K}_2\text{CO}_3$  particles are the main components of smoke at  $Y(\text{S}) < 14 \text{ wt\%}$ , and have an average diameter of  $\sim 400 \text{ nm}$ , whereas  $\text{K}_2\text{SO}_4$  particles are dominant at  $Y(\text{S}) > 14 \text{ wt\%}$  and have an average diameter of  $400\sim 500 \text{ nm}$ , as depicted in Figure 7(A). Although the main component of the smoke changes from  $\text{K}_2\text{CO}_3$  to  $\text{K}_2\text{SO}_4$  according to the mass fraction of sulfur, the total volume fraction (sum of the volume fractions of  $\text{K}_2\text{CO}_3$  and  $\text{K}_2\text{SO}_4$ ) is greater than  $1 \times 10^{-4}$ , as depicted in Figure 7(B). We conclude that a very large amount of smoke composed of  $\text{K}_2\text{CO}_3$  or  $\text{K}_2\text{SO}_4$  will be produced from black powder combustion. The predictions in Figure 7 are qualitatively equivalent to the CNT predictions illustrated in Figure 5.

#### 4. Effects of addition of ammonium perchlorate ( $\text{NH}_4\text{ClO}_4$ , AP) to the black powder

The above arguments predict that the smoke from black powder combustion is composed of potassium salts and that a very large amount of smoke should be produced. In this section, a strategy for reducing the smoke particles will be discussed. Since the smoke particles are composed of potassium salts, reducing the potassium in the black powder recipe should reduce the number of smoke particles. Potassium in black powder comes from the oxidizer,  $\text{KNO}_3$ . Therefore, the replacement of  $\text{KNO}_3$  with another oxidizer that does not include potassium, such as  $\text{NH}_4\text{NO}_3$  (ammonium nitrate, AN) or  $\text{NH}_4\text{ClO}_4$ , AP, should reduce the amount of smoke

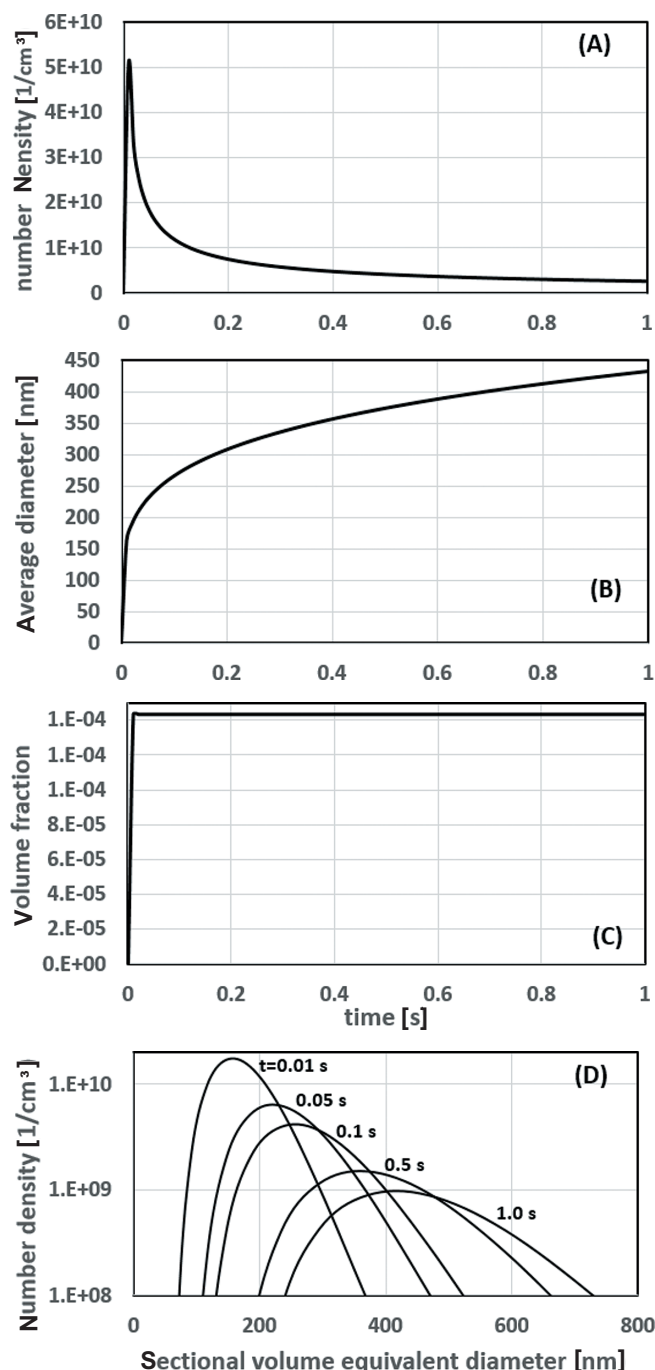


**Figure 6** Time history of number density (A), average particle diameter (B), volume fraction (C) and particle-size distribution (D) of  $\text{K}_2\text{CO}_3$  particles formed in black powder combustion obtained by solving Smoluchowski equation. Composition of black powder:  $\text{C/S/KNO}_3 = 15/10/75 \text{ wt\%}$ ,  $P = 1 \text{ bar}$  and partial equilibrium temperature is  $T = 1181 \text{ K}$ .

produced. We consider the addition of AP to black powder. Addition of AP will result in a higher adiabatic temperature for the combustion process. CNT predicts that this increased combustion temperature will result in the reduction of smoke, because of the higher vapor pressure of precursor molecules for smoke-particle formation. This increased vapor pressure reduces the supersaturation ratio,  $\xi$ , and thereby increases the critical radius (see Equation(2)).

The complete chemical equilibrium composition and adiabatic temperatures at  $P = 1 \text{ bar}$  are illustrated in

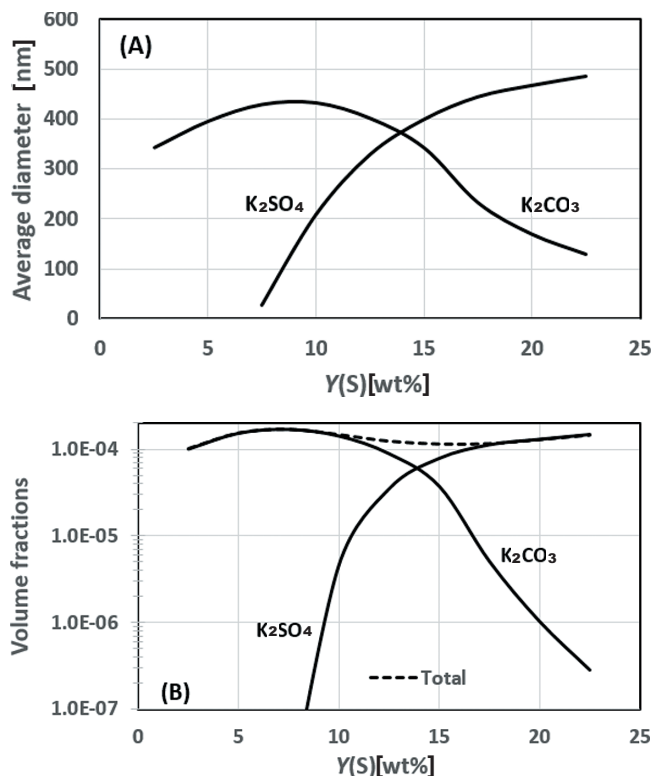


Figure 7 Average diameter (A) and volume fraction (B) of  $K_2CO_3$  and  $K_2SO_4$  smoke particle at  $t=1$  sec after the partial equilibrium obtained by solving Smoluchowski equation as a function of  $Y(S)$ . Conditions are same as in Figure 3.

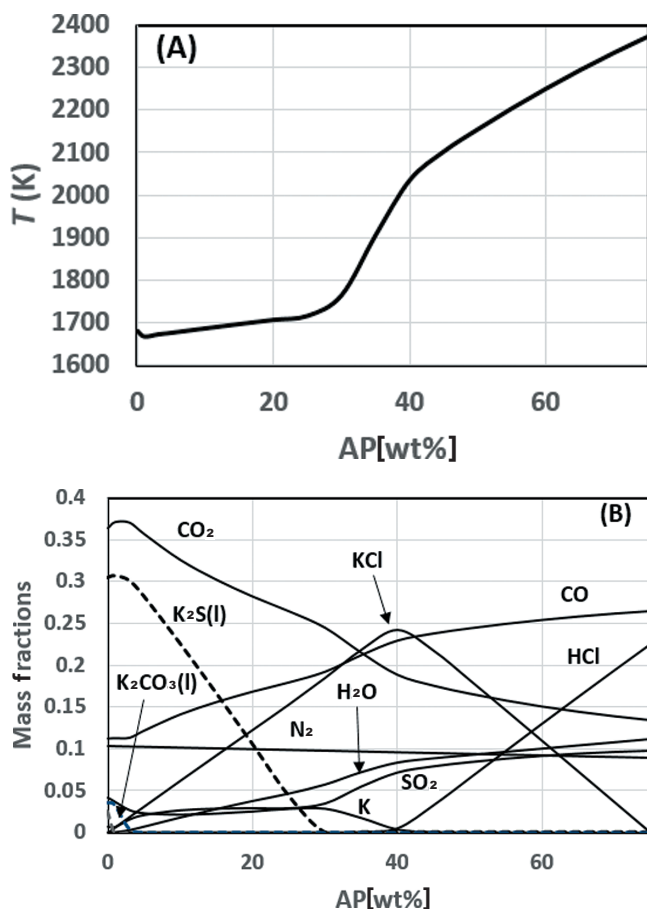


Figure 8 Equilibrium temperature (A) and compositions (B) of black powder combustion at constant pressure ( $p=1$  bar) and adiabatic condition as a function of mass fraction of AP. Composition of black powder: C/S/ $KNO_3$ /AP=15/10/75-X/X wt%.

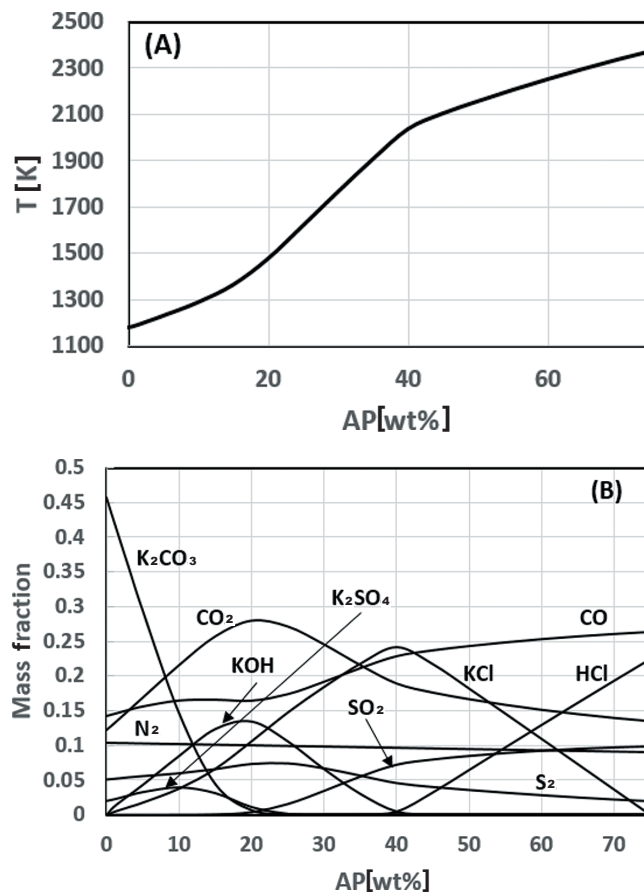


Figure 9 Partial equilibrium temperature (A) and compositions (B) of black powder combustion at constant pressure ( $p=1$  bar) and adiabatic condition as a function of mass fraction of AP. Composition of black powder: C/S/ $KNO_3$ /AP=15/10/75-X/X wt%. Chemical species in condensed phase are excluded in this calculation.

Figure 8 for the black powder recipe C/S/ $KNO_3$ /AP = 15/10/75-X/X wt%.

Adiabatic temperature slightly decreases with a small AP addition (less than 5 wt%) and increases with increasing amounts of added AP. Especially, the temperature increase is very large with an AP addition of 30–40 wt%. The main solid products are  $K_2S(l)$ ,  $K_2CO_3(l)$ , and  $K_2SO_4(l)$ . Note that the fractions of  $K_2CO_3(l)$  and  $K_2SO_4(l)$  are greatly reduced by the addition of AP, but the fraction of another potassium salt in the gas phase,  $KCl$ , increases for additions up to 40 AP wt%.

To determine the initial conditions for smoke generation of black powder with added AP, partial-equilibrium calculations without condensed chemical species were performed. The results are depicted in Figure 9. The partial-equilibrium temperature considerably increases with the addition of AP. With the composition of 15 wt% C and 10 wt% S, the mass fraction of  $K_2SO_4$  is quite low. The mass fraction of  $K_2CO_3$  rapidly decreases with increasing additions of AP. However, the fraction of another potassium salt,  $KCl$ , increases with additions of AP up to 40 wt%. This indicates that  $KCl$  smoke particles may be formed when AP is added.

To estimate the formation of  $KCl$  particles with CNT and the Smoluchowski equation, data on vapor pressure, surface tension, and density of condensed phase are



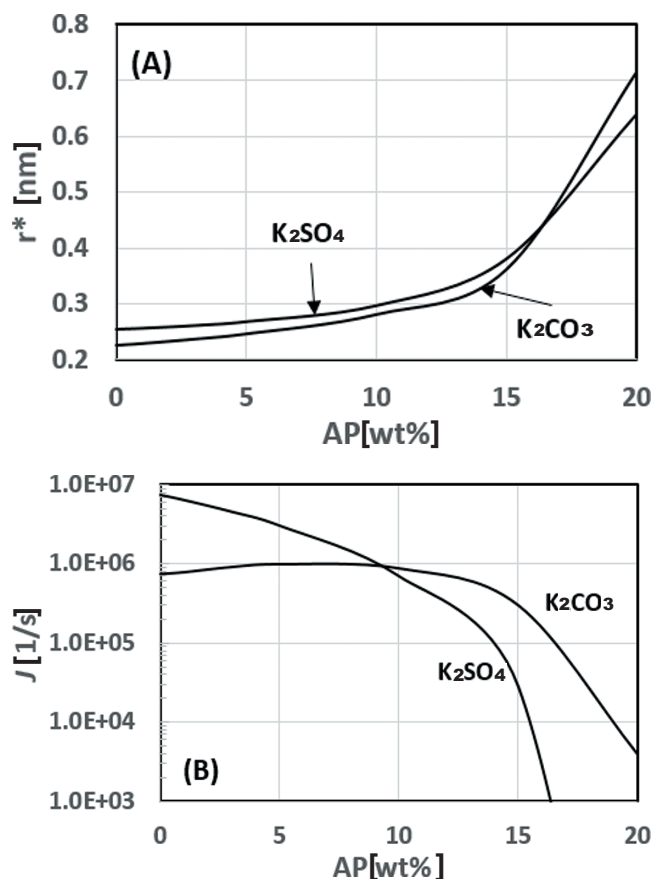


**Figure 10** Critical radius and rate of nucleation,  $J$ , for  $K_2CO_3$  and  $K_2SO_4$  in black powder combustion as a function of added AP wt% (X). Composition of black powder: C/S/ $KNO_3$ /AP=15/10/75-X/X wt%.

required. The vapor pressure of KCl is calculated based on thermochemical data given in the CEA database<sup>16)</sup>, and is depicted in Figure 4. Note that the vapor pressure of KCl is much higher than that of  $K_2CO_3$  or  $K_2SO_4$ . The vapor pressure for KCl in bars can be expressed as:

$$\ln P_{eq} (KCl) = -25815.9/T + 16.99, \quad 500 \leq T \leq 1044K$$

$$= -18953.2/T + 10.74, \quad T \geq 1044K$$

The melting point is 1044 K. The density of KCl is given in Reference 20) as:

$$\rho (KCl) = 2.1359 - 5.831 \times 10^{-4} T. \quad [g \text{ cm}^{-3}]$$

The surface tension of KCl is taken from Reference 21):

$$\sigma (KCl) = 177.61 - 0.07519 T. \quad [mN \text{ m}^{-1}]$$

Because of the very high vapor pressure of KCl, the value of  $\xi$  is greater than 1 at the region of X (wt% of AP) > 20 wt%. Even at X < 20 wt%, the critical radius of KCl is too large for nucleation to occur (on the order of 0.1 mm). As a result, CNT does not predict the formation of KCl particles; rather  $K_2CO_3$  and  $K_2SO_4$  particles would be produced. These results are depicted in Figure 10.

The critical radii of  $K_2CO_3$  and  $K_2SO_4$  particles are less than 0.4 nm at X < 15 wt% and rapidly increase after X > 15 wt%. The nucleation rates of  $K_2CO_3$  and  $K_2SO_4$  also rapidly decrease after X > 15 wt%. These results indicate that the addition of AP to a standard black powder recipe will greatly suppress the generation of smoke particles.

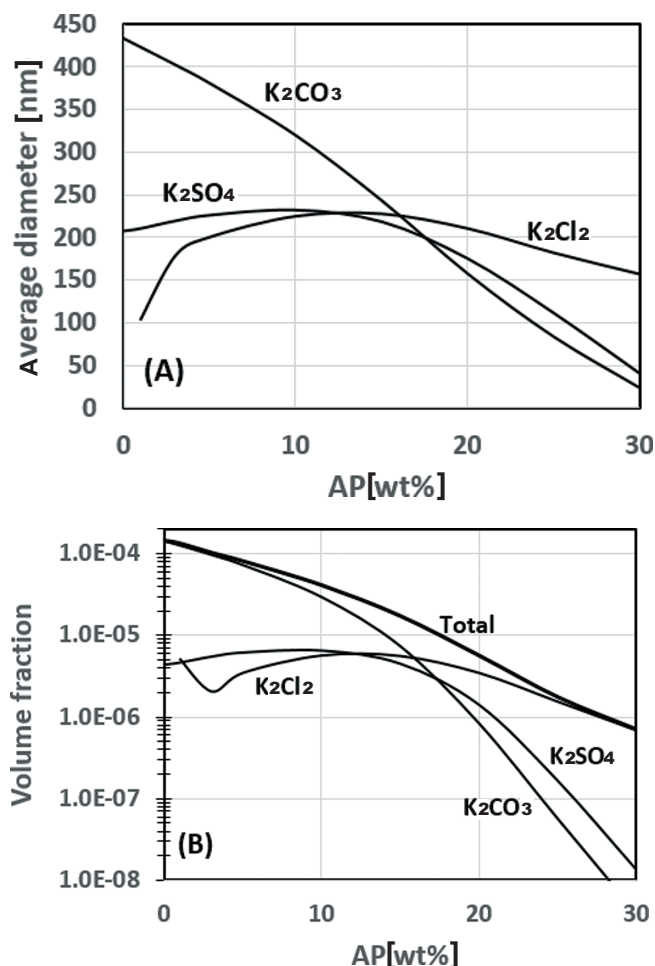


**Figure 11** Average diameter (A) and volume fraction (B) of smoke particles at  $t=1\text{sec}$  after the partial equilibrium obtained by solving Smoluchowski equation as a function of added AP wt% (X). Composition of black powder: C/S/ $KNO_3$ /AP=15/10/75-X/X wt%.

The effect of AP addition is predicted to be remarkable if X > 15 wt%.

Contrary to CNT, solution of the Smoluchowski equation predicts the production of KCl particles, if we can define the particle-inception reactions for KCl. Partial-equilibrium calculations indicate that the mass fraction of KCl increases with an increasing X, as depicted in Figure 9. In the case of  $K_2CO_3$  and  $K_2SO_4$ , we assumed that the minimum size of the particle is  $j = 2$ . However, in the case of KCl, partial-equilibrium calculations demonstrate the existence of a dimer of KCl,  $K_2Cl_2$ , as a gas-phase chemical species, although its concentration is quite low. Because of this, we assume the following KCl particle-inception reactions:



Reaction (R9) is the recombination reaction of KCl in the gas phase and M is a third body. The particle-inception reaction is reaction (R10), that indicates the minimum size of KCl particles is  $j = 4$ . Since there is no available data about the rate coefficients for (R9) and (R10), the rate coefficient of Cl recombination is assumed for reaction (R9) and the following collision rate is assumed for reaction (R

10);

$$k_{R10} = 8.67 \times 10^{12} T^{0.5} \text{ [cm}^3\text{mol}^{-1}\text{s}^{-1}\text{]}$$

The average diameters and volume fractions of  $\text{K}_2\text{CO}_3$ ,  $\text{K}_2\text{SO}_4$ , and KCl as predicted by solutions of the Smoluchowski equation are depicted in Figure 11 for the black powder recipe  $\text{C/S/KNO}_3/\text{AP} = 15/10/75\text{-X/X wt\%}$ . The values are plotted as a function of X.

The main component of smoke at  $X < 16 \text{ wt\%}$  is  $\text{K}_2\text{CO}_3$  particles, while it changes to KCl particles at  $X > 16 \text{ wt\%}$ , and the average diameter of smoke particles decreases from 440 nm at  $X = 0$  to 160 nm at  $X = 30 \text{ wt\%}$ , as depicted in Figure 11(A). The total volume fraction decreases by two orders of magnitude with the addition of 30 wt% AP, as illustrated in Figure 11(B). These results suggest that the addition of AP to a standard black powder recipe can greatly reduce the generation of smoke particles.

## 5. Concluding remarks

This study develops a novel model to predict smoke formation in black powder combustion. CNT predicted that standard black powder with 75 wt% of  $\text{KNO}_3$  produces smoke particles very quickly, as the time constant of nucleation is less than 1  $\mu\text{s}$ . The composition of the smoke particles depends on the mass fraction of sulfur in the black powder.  $\text{K}_2\text{CO}_3$  is the main component of the smoke from a sulfur-lean mix, and  $\text{K}_2\text{SO}_4$  is dominant in the smoke from sulfur-rich black powder. The time variations of particle-size distribution, average diameter, and volume fraction of smoke particles are also estimated by solving the Smoluchowski equation. 400-nm-diameter smoke particles at a volume fraction of  $10^{-4}$  are predicted to be produced by the combustion of standard black powder.

We also use CNT and the Smoluchowski equation to predict the effects of adding AP to the black powder. CNT predicted that critical radii of  $\text{K}_2\text{CO}_3$  and  $\text{K}_2\text{SO}_4$  particles can be considerably increased by the addition of AP. Although CNT predicted that no KCl particles will be formed, the Smoluchowski equation indicates that KCl particles will be produced with a large addition of AP. Solutions of the Smoluchowski equation indicate that the average particle diameter and the volume fraction of smoke decrease when increasing the amount of added AP. Thus, adding AP to standard black powder may be very effective to reduce smoke formation. It is highly desirable this prediction is validated by the experiments in future. Data on the composition of smoke particles is especially interesting.

In the present model, many assumptions were used because of the lack of experimental data on the properties of the smoke formed in black powder combustion. Therefore, results obtained in the present study are not expected to be quantitative. Clearly experimental data is required to validate present results. Especially, data on the composition of smoke particle is highly desirable.

Several other problems remain with the present model of smoke formation. They are listed below.

(1) The nucleation of  $\text{K}_2\text{S}$  is not included in the present

model. This is because of a lack of available data about  $\text{K}_2\text{S}$  particle formation. As depicted in Figure 1, a large amount of liquid  $\text{K}_2\text{S}$  is produced at complete equilibrium. Therefore, smoke particles must include  $\text{K}_2\text{S}$  nuclei. However, no evidence of the existence of gas-phase  $\text{K}_2\text{S}$  is available and therefore,  $\text{K}_2\text{S}$  nuclei cannot be formed by nucleation from  $\text{K}_2\text{S}$  gas molecules. Nucleation of  $\text{K}_2\text{S}$  may proceed via some other chemical reactions, which should be studied in the future.

(2) In this study, the partial pressures of precursor molecules are estimated with partial-equilibrium calculations. This estimation gives the maximum partial pressure of the precursor since many liquid-phase reactions of the same species might simultaneously proceed. For more-precise predictions, detailed models of the liquid-phase reactions are needed in addition to our model of gas-phase reactions.

(3) The critical radius of potassium salt particles is comparable to the radius of a single molecule. This indicates the failure of the capillary approximation in CNT<sup>7), 22)</sup>. More sophisticated models, such as the kinetic Monte Carlo method<sup>23)</sup>, may be useful for modeling smoke formation in detail.

This study is the first step toward modeling smoke formation in fireworks. Future studies will continue to work toward controlling smoke generation in fireworks.

## References

- 1) R. Vecchi, V. Bernardoni, D. Cricchio, A. D'Alessandro, P. Fermo, F. Lucarelli, S. Nava, A. Piazzalunga, and G. Valli, *Atmospheric Environment*, 42, 1121–1132 (2008).
- 2) M.R. Sijimol and M. Mohan, *Environ. Monit. Assess.*, 186, 7203–7210 (2014).
- 3) Q. Jtang, Y.L. Sun, Z. Wang, and Y. Yin, *Atmospheric Chemistry and Physics*, 15, 6023–6034 (2015).
- 4) D.J. Seidel and A.N. Birnbaum, *Atmospheric Environment*, 115, 192–198 (2015).
- 5) M. Jumar, R.K. Singh, V. Murari, A.K. Singh, R.S. Singh, and T. Banmerjee, *Atmos. Res.*, 180, 78–91 (2016).
- 6) R. Camilleri and A.J. Vella, *Propellants, Explosives, and Pyrotechnics*, 41, 273–280 (2016).
- 7) S. Karthika, T.K. Radhakrishnan, and P. Kalaichelvi, *Cryst. Growth Des.*, 16, 6663–6681 (2016).
- 8) B.E. Wyslouzil and J. Wolk, *J. Chem. Phys.*, 145, 211702 (2016).
- 9) S.L. Girshick and C-P. Chiu, *J. Chem. Phys.*, 93, 1273–1277 (1990).
- 10) M. Frenklach, *Chem. Eng. Sci.*, 57, 2229–2239 (2002).
- 11) ANSYS 18.1 Chemkin-Pro Theory manual, Chap. 18, ANSYS, INC., San Diego, (2017).
- 12) J.D. Litster, D.J. Smit, and M.J. Hounslow, *AIChE J.* 41, 591–603 (1995).
- 13) S. Kumer and D. Ramkrishna, *Chem. Eng. Sci.*, 52, 4659–4679 (1997).
- 14) M.S. Russell, "The Chemistry of Fireworks," Chap.2, The Characteristics of Black Power, 2nd Ed., The Royal Society of Chemistry, Cambridge, UK (2009).
- 15) J.A. Conkling and C. Mocella, "Chemistry of Pyrotechnics," 2nd Ed., CRC Press, Taylor & Francis Group, New York (2010).

- 16) B.J. McBride and S. Gordon, "Computer Program for Calculation of Complex Chemical Equilibrium Compositions and Applications," NASA Reference Publication 1311 (1994).
- 17) H. Watanabe, K. Shimomura, and K. Okazaki, *Energy Fuels*, 28, 4795–4800 (2014).
- 18) L.L. Simmons, L.F. Lowden, and T.C. Ehlert, *Chem. Phys.*, 81, 706–709 (1977).
- 19) D.A. McQuarrie and J.D. Simon, "Physical Chemistry-A Molecular Approach," Chap.23, University Science Books (1997).
- 20) G.J. Janz, *J. of Physical and Chemical Reference Data*, vol.17 supplement No.2 (1988).
- 21) W.M. Hayes, Editor-in-Chief, "Handbook of Chemistry and Physics," 97th Ed., CRC Press, New York (2016–2017).
- 22) S.L. Girshick, *J. Chem. Phys.*, 141, 024307 (2014).
- 23) A. Fillipponi and P. Giammatteo, *J. Chem. Phys.*, 145, 211913 (2016).